

Highly Sensitive Surface Acoustic Wave NH₃ Gas Sensor Based on TiO₂ Film

Lei Zhao,^{1*} Ruili Wang,² and Qingqing Cao¹

¹Nanjing Vocational University of Industry Technology, Nanjing, 210023, P.R. China

²Massey University, Private Bag 11222, Palmerston North 4442, New Zealand

(Received October 8, 2020; accepted November 16, 2020)

Keywords: surface acoustic wave, NH₃, gas sensor, hydroxyl group

We fabricated a surface acoustic wave (SAW) NH₃ gas sensor based on a TiO₂ sensitive film. The TiO₂ film was deposited using a combined sol-gel and spin-coating technology. Scanning electron microscopy (SEM) and X-ray diffraction (XRD) results indicate that the film was porous and had good crystallinity. Fourier Transform infrared spectroscopy (FTIR) analysis revealed that there was a large amount of hydroxyl groups on the film, which can capture H₂O molecules from the ambient environment. The sensor showed a positive response to NH₃ gas and the response increased significantly with increasing relative humidity. The positive response was found to be caused by the change in the elastic modulus of the sensitive film, which was induced by the condensation of the hydroxyl groups on the film catalyzed by NH₃. The sensor also had a low detection limit of 1 ppm and excellent selectivity and stability to NH₃ gas.

1. Introduction

NH₃, an important industrial gas, is widely used in some traditional industrial fields such as fertilizers, rubber, and refrigeration.^(1–4) In addition, NH₃ plays a critical role in some advanced areas of semiconductor technology, such as the LED and solar cell manufacturing industries.^(5–7) It is also a source of atmospheric pollution and can cause various respiratory diseases even at low concentrations.^(8–10) Furthermore, when the concentration of NH₃ is higher than 500 ppm, it can even cause death.⁽¹¹⁾ Therefore, continuous monitoring of the concentration of NH₃ gas in factories and living spaces is extremely important.

Sensors based on various techniques have been used for NH₃ monitoring, such as electrochemical sensors,⁽¹²⁾ semiconductor sensors,^(13,14) and surface acoustic wave (SAW) sensors.⁽¹⁵⁾ Among these sensors, SAW sensors have the advantages of high sensitivity, reliability, and accuracy. These advantages are due to the fact that any physical and chemical changes on the surface of the SAW device can induce a perturbation of the velocity of a SAW, which leads to changes in the working frequency of the SAW sensor.⁽¹⁶⁾ To further enhance the sensitivity of SAW gas sensors, sensitive films are usually deposited on the devices. Upon

*Corresponding author: e-mail: 2014100795@niit.edu.cn
<https://doi.org/10.18494/SAM.2020.3139>

exposure to tested gases, the films may react with the gases. As a result, the conductivity, weight, and elastic modulus of the sensitive film may change, resulting in the response of the sensor.^(17–21)

Different materials have been used as the sensitive films of SAW NH₃ sensors. For example, Chen *et al.*⁽²²⁾ reported a sensitive SAW NH₃ gas sensor based on a Pt-doped polypyrrole sensitive film and Su *et al.*⁽²³⁾ reported a NH₃ gas sensor based on a Pd/SnO₂/RGO ternary composite that operated at room temperature. Among the materials used for sensitive films, TiO₂ has been widely used and studied because of its chemical sensitivity, high thermal and chemical stabilities, amenability to doping, nontoxicity, and low cost.^(24–26) Nevertheless, the sensing mechanism of a SAW sensor with a TiO₂ sensitive film has not been revealed yet.

In this study, we fabricated a SAW NH₃ gas sensor based on a TiO₂ sensitive film. This sensor had a detection limit of 1 ppm, as well as excellent selectivity and stability. The sensing mechanism of the sensor was investigated. It was found that the positive responses of the sensor were caused by the change in the elastic modulus of the sensitive film, which was induced by the condensation of the hydroxyl groups on the film catalyzed by NH₃.

2. Experimental Details

The SAW device used in this work was a two-port resonator based on a ST-cut quartz substrate. Interdigital transducers (IDTs) and reflecting gratings were deposited on both ends of the quartz substrate. The period of the IDTs and gratings was 16 μm, as shown in Fig. 1, and the velocity of a SAW propagating on the resonator was 3158 m/s. Thus, the working frequency of the uncoated resonator was ~200.102 MHz. The insertion loss and the Q factor of the resonator measured by a vector network analyzer (VNA) were ~9.45 dB and ~7000, respectively, as shown in Table 1.

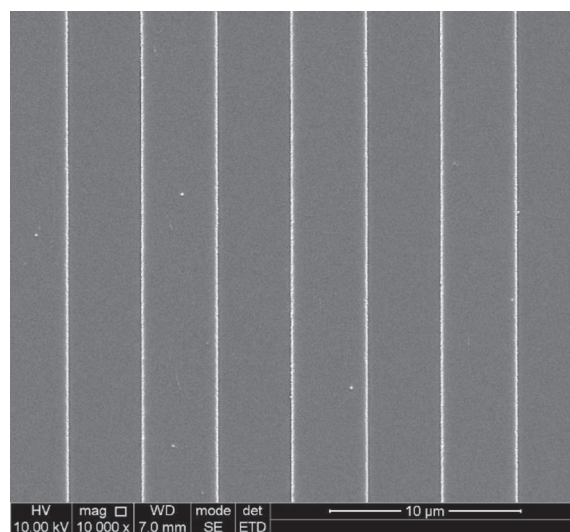


Fig. 1. Structure of the IDTs on the quartz substrate.

Table 1

Insertion loss, working frequency, and Q factor of the SAW resonator before and after coating with TiO₂ film.

Sample	Insertion loss (dB)	Working frequency (MHz)	Q factor
Pristine resonator	9.45	200.102	7000
Resonator coated with TiO ₂ film	19.46	199.325	2300

The TiO₂ film was deposited onto the SAW resonator using a combined sol-gel and spin-coating technology. Tetrabutyl titanate was first added to a beaker containing ethanol under magnetic stirring for 30 min, and then ammonia (25–28 wt%) was added to the beaker dropwise under vigorous stirring. The obtained solution was then aged for 1 day to obtain the colloidal TiO₂ sol. The TiO₂ sol was coated onto the SAW resonator using a spin-coating technique with a speed of 3000 rev/min for 30 s. The coated quartz resonator was annealed at 300 °C for about 1 h in air.

Compared with the pristine resonator, the annealed resonator had a decreased working frequency of 199.325 MHz, which was caused by the mass of the TiO₂ film loaded on the resonator. The coated resonator also had a higher insertion loss of ~19.46 dB and a lower Q factor of ~2300, as shown in Table 1.

The coated resonator was used as a frequency selector to build a SAW oscillator with a cascaded amplifier having a gain of 40 dB and a phase shift network consisting of capacitors and inductors, as shown in Fig. 2. The oscillating frequency was recorded as the output signal of the SAW sensor using a frequency counter (HP5385A), and the response of the sensor was defined as the frequency shift, $\Delta f = f_s - f_0$, where f_s is the oscillating frequency of the sensor in the tested gas and f_0 is the frequency in pure air.

The responses of the sensor to different gases were measured using the experimental setup shown in Fig. 2. The sensor was placed in a chamber with a volume of 20 L. The tested gases (NH₃, H₂, CH₄, CO, ethanol, and SO₂) were injected into the chamber with a syringe to investigate the response of the sensor. The concentration of the tested gases in the chamber was controlled by adjusting the amount of the tested gases injected. When the response of the sensor reached a stable value, the chamber was opened to expose it to pure air to allow the recovery of the sensor.

The crystallinity of the prepared films was characterized by an X-ray diffractometer (XRD, Rigaku D/max-2400). The morphology and thickness of the as-prepared films were characterized by a field-emission scanning electron microscope (SEM, FEI Inspect F). An FTIR spectrometer (Nicolet 6700) was used to collect the infrared transmission spectra of prepared films. A VNA (Agilent Technologies, E8363B) was used to characterize the transmission properties of the pristine and coated SAW resonators.

3. Results and Discussion

The XRD pattern of the prepared TiO₂ is shown in Fig. 3. Peaks located at $2\theta = 25.4, 38, 47.9, 54.4, \text{ and } 63^\circ$ were observed. These peaks were assigned to the diffraction signals of (101), (004), (200), (105), and (204) planes of rutile TiO₂, respectively. This result indicates that the film had high crystallinity.

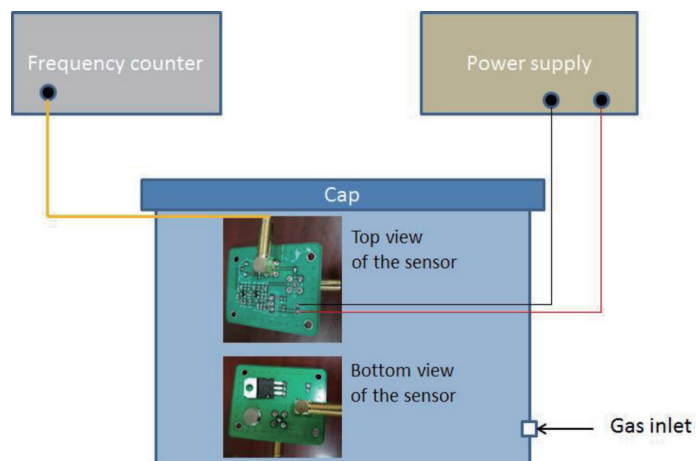


Fig. 2. (Color online) Experimental setup for the gas sensing test.

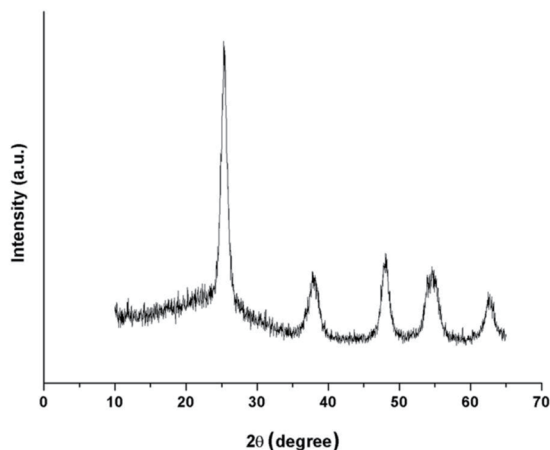


Fig. 3. XRD pattern of the TiO_2 film.

SEM images of the TiO_2 film are shown in Fig. 4. The film consisted of TiO_2 nanoparticles with a diameter of ~ 15 nm. In addition, it was found that there are some open pores in the film, which provide paths for gas to diffuse in and out from the films. These pores are beneficial for the gas sensor application.

The FTIR result of the TiO_2 film is shown in Fig. 5. Two broad bands at 3490 and 1640 cm^{-1} were observed, which are the stretching and bending modes of absorbed water, respectively. The broad and intense band in the range of $400\text{--}800\text{ cm}^{-1}$ was assigned to Ti–O and Ti–O–Ti groups. The band at 3737 cm^{-1} was ascribed to surface Ti–OH groups and the band ranging from 1300 to 1500 cm^{-1} was assigned to the residual carbon. This FTIR result indicates that there were abundant hydroxyl groups that absorbed water on the film.

Figure 6 shows the sensing performances of the sensor to 10 ppm NH_3 at room temperature and RH = 10, 50, and 80%. The response of the sensor was significantly enhanced with

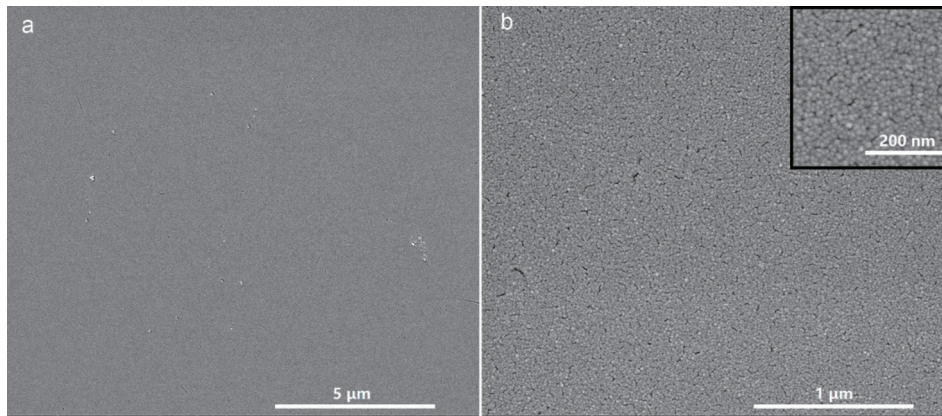


Fig. 4. SEM images of the TiO₂ film with different magnifications. (a) 20000× and (b) 100000×. Inset in (b) shows that the particle size of the film is ~15 nm.

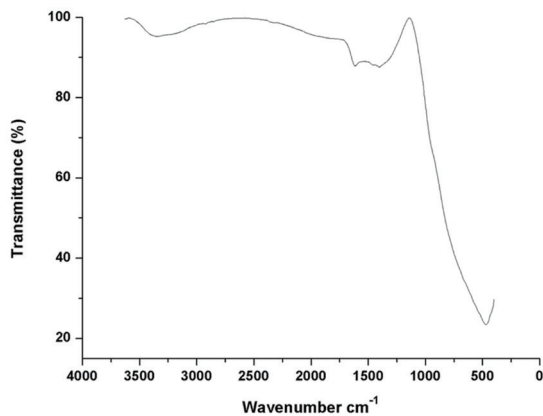


Fig. 5. FTIR result of the TiO₂ film.

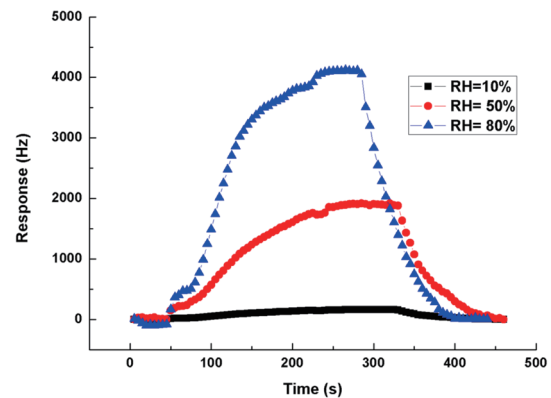


Fig. 6. (Color online) Responses of the sensor with TiO₂ film to 10 ppm NH₃ gas at different RH values.

increasing RH value and reached 4200 Hz at RH = 80%. It has been established that the response of a SAW gas sensor is derived from three effects occurring on the film, i.e., those of mass loading, elastic loading, and conductivity loading, which refer to the changes in weight, elastic modulus, and conductivity of the sensing film, respectively.^(16–21) Previous research has revealed that the conductivity loading effect contributes little to the response of a SAW sensor based on an insulating sensitive layer.⁽¹⁸⁾ Therefore, in this work, the mass loading and elastic loading effects are the two possible mechanisms dominating the responses of the sensor.

When the sensor is exposed to NH₃ gas, NH₃ may adsorb on the surface and in the pores of the TiO₂ film. The adsorbed NH₃ can first lead to an increase in the weight (mass loading effect) of the film. Furthermore, the NH₃ can also lead to condensation between the hydroxyl groups on the film by acting as a catalyst, as shown in Fig. 7.^(26,27) This condensation may enhance the stiffness of the film, finally resulting in an increase in the elastic modulus (elastic modulus effect) of the film. According to previous reports,^(16–21) the mass loading effect leads

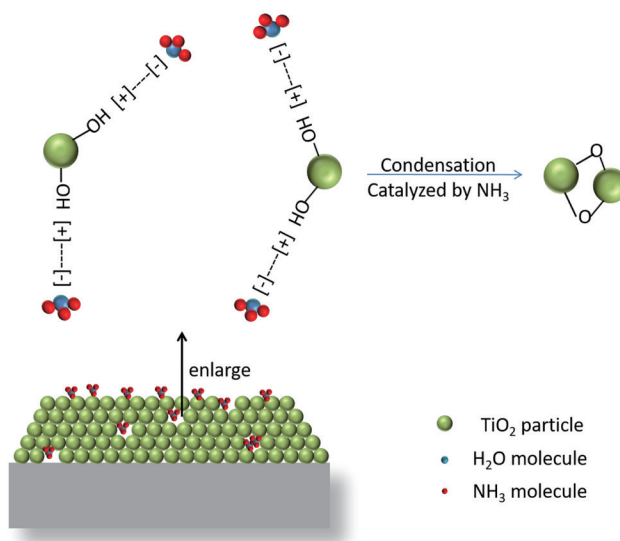


Fig. 7. (Color online) Proposed sensing mechanism of the sensor with TiO₂ film.

to a negative response while the elastic loading effect leads to a positive response in this case. Hence, it was concluded that the positive responses of the sensor at different RH values were dominated by the elastic loading effect.

The reason for the different responses at different RH values was further investigated. The FTIR result revealed that there were abundant hydroxyl groups on the TiO₂ film. These hydroxyl groups can effectively capture H₂O molecules from the ambient environment by the formation of hydrogen bonds, as shown in Fig. 7, and the amount of H₂O captured by the film is dependent on the ambient humidity; with increasing humidity, the amount of H₂O increases. NH₃ has a good affinity to H₂O; therefore, when the film is exposed to NH₃ gas, NH₃ molecules can be captured by H₂O, as shown in Fig. 7. Thus, the amount of NH₃ captured is related to the RH value. At a low RH (10%), the amount of NH₃ captured by hydroxyl groups is relatively small, while at a high RH (80%), a large amount of NH₃ is captured. As a result, more NH₃ acts as the catalyst for the condensation reaction between the hydroxyl groups at a higher RH, leading to a stiffer film and a stronger positive response of the sensor.

Although the sensor had the best performance at RH = 80%, such a sensor would normally be used in an ambient environment with an RH value around 50%. Thus, all the following tests related to the sensitivity, selectivity, and stability of the sensor were conducted at RH = 50%. Figure 8 shows the dynamic response of the sensor to 1–100 ppm NH₃ gas. The sensor had a response frequency of 500 Hz to 1 ppm NH₃, and the response frequency increased with the concentration of NH₃, reaching 3200 Hz when the concentration was 100 ppm. The selectivity of the sensor was also investigated by exposing it to different gases. As shown in Fig. 9(a), the sensor showed no response to H₂, CO, CH₄, and ethanol gases with a concentration of 100 ppm. When exposed to SO₂ gas, the sensor exhibited a slight positive response. This positive response may also have originated from the condensation of hydroxyl groups since SO₂ can also

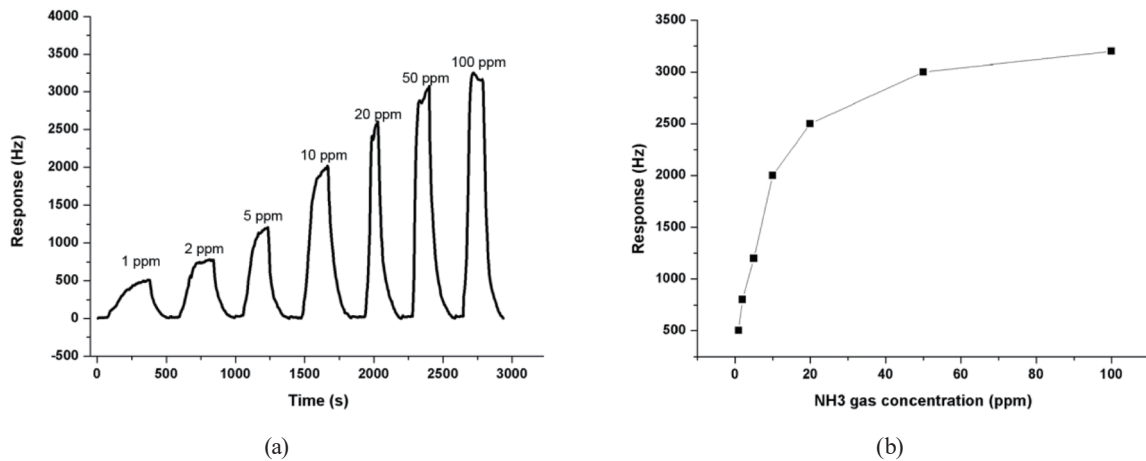


Fig. 8. (a) Dynamic response of the sensor to NH₃ gas with different concentrations; (b) response of the sensor as a function of the NH₃ concentration.

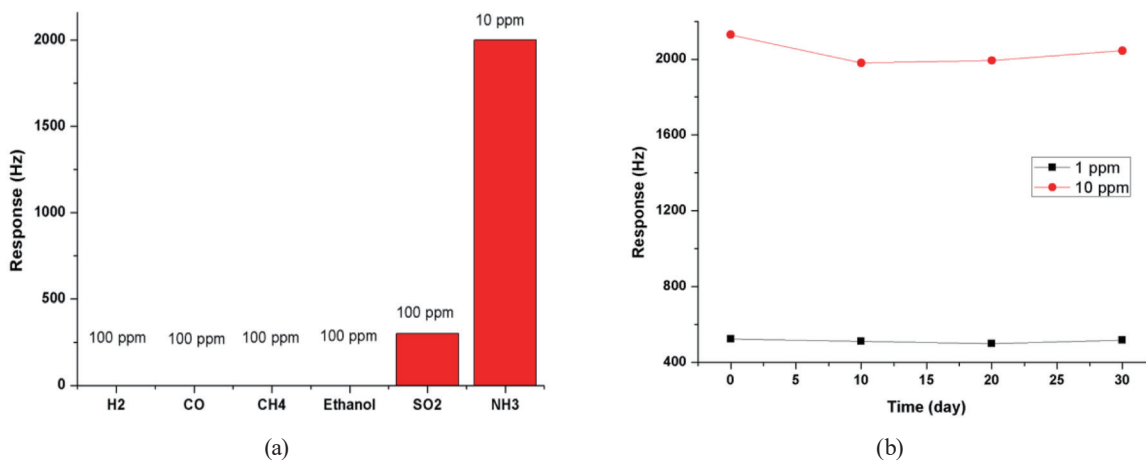


Fig. 9. (Color online) (a) Response of the sensor to different gases; (b) responses of the sensor to 1 and 10 ppm NH₃ gas over 30 days.

act as a catalyst for the condensation reaction. However, the positive response to SO₂ was much weaker than that to NH₃. Thus, the sensor had excellent selectivity to NH₃ gas. The stability of the sensor was further investigated by conducting five tests over 30 days. As shown in Fig. 9(b), this sensor had similar responses to 1 and 10 ppm NH₃ gases throughout the 30 days, indicating its good stability.

4. Conclusion

A SAW NH₃ sensor based on a TiO₂ sensitive film was fabricated. Its response to NH₃ gas was enhanced significantly with increasing RH value and reached 4200 Hz (10 ppm NH₃) at

RH = 80%. This enhancement is due to the fact that more NH₃ molecules are captured by H₂O absorbed on the film at a higher RH. The sensing mechanism of the sensor was found to be dominated by the change in the elastic modulus of the sensitive film, which was caused by the NH₃-catalyzed condensation between the hydroxyl groups on the film. The sensor also showed excellent selectivity and stability to NH₃ gas, indicating its potentially practical application.

Acknowledgments

The authors acknowledge the Jiangsu Intelligent Sensor Network Open Fund (ZK16-02-04). This study is supported by Jiangsu Government Scholarship.

Declaration of Interest

The author(s) declare that they have no competing interests.

References

- 1 L. Yu'e and L. Erda: *Nutr. Cycl. Agroecosyst.* **57** (2000) 99. <https://doi.org/10.1023/A:1009828705104>
- 2 N. Hu, Z. Yang, Y. Wang, L. Zhang, Y. Wang, X. Huang, H. Wei, L. Wei, and Y. Zhang: *Nanotechnology* **25** (2013) 025502. <https://doi.org/10.1088/0957-4484/25/2/025502>
- 3 N. Peng, Q. Zhang, C. L. Chow, O. K. Tan, and N. Marzari: *Nano Lett.* **9** (2009) 1626. <https://doi.org/10.1021/nl803930w>
- 4 J. Gong, Y. Li, Z. Hu, and Y. Deng: *J. Phys. Chem. C* **114** (2010) 9970. <https://doi.org/10.1021/jp100685r>
- 5 N. Okada, F. Ishida, Y. Mitsui, K. Tadatomo, Hi. Mangyo, Y. Kobayashi, H. Ono, K. Ikenagai, Y. Yano, and K. Matsumoto: *Jan. J. Appl. Phys.* **48** (2009) 062102. <https://doi.org/10.1143/JJAP.48.062102>
- 6 X. Wang, Y. Yang, Z. Jiang, and R. Fan: *Eur. J. Inorg. Chem.* **23** (2009) 3481. <https://doi.org/10.1002/ejic.200900134>
- 7 Y. H. Wu, L. L. Chen, J. R. Wu, and M. L. Wu: *Semicond. Sci. Technol.* **25** (2009) 015001. <https://doi.org/10.1088/0268-1242/25/1/015001>
- 8 A. Kumar, R. S. Patil, A. K. Dikshit, and R. Kumar: *Asian J. Atmos. Environ.* **13** (2019) 1. <https://doi.org/10.5572/ajae.2019.13.1.011>
- 9 C. D. Koolen and G. Rothenberg: *ChemSusChem* **12** (2019) 164. <https://doi.org/10.1002/cssc.201802292>
- 10 M. Gomzi and M. Šarić: *Int. Arch. Occ. Env. Health* **70** (1997) 314. <https://doi.org/10.1007/s004200050224>
- 11 Y. Wang, J. Liu, X. Cui, Y. Gao, J. Ma, Y. Sun, P. Sun, F. Liu, X. Liang, T. Zhang, and G. Lu: *Sens. Actuators, B* **238** (2017) 473. <https://doi.org/10.1016/j.snb.2016.07.085>
- 12 X. Ji, C. E. Banks, D. S. Silvester, L. Aldous, C. Hardacre, and R. G. Compton: *Electroanalysis* **19** (2007) 2194. <https://doi.org/10.1002/elan.200703997>
- 13 D. J. Late, T. Doneux, and M. Bougouma: *Appl. Phys. Lett.* **105** (2014) 233103. <https://doi.org/10.1063/1.4903358>
- 14 K. Shingange, Z. P. Tshabalala, O. M. Ntwaeaborwa, D. E. Motaunga, and G. H. Mhlongo: *J. Colloid Interf. Sci.* **479** (2016) 127. <https://doi.org/10.1016/j.jcis.2016.06.046>
- 15 I. Constantinoiu, D. Miu, and C. Viespe: *J. Sensors* **2019** (2019). <https://doi.org/10.1155/2019/8203810>
- 16 D. S. Ballantine Jr., R. M. White, S. J. Martin, A. Ricco, E. T. Zellers, G. C. Frye, and H. Wohljen: *Acoustic Wave Sensors: Theory, Design and Physico-chemical Applications* (Elsevier, 1996).
- 17 M. Thompson and D. C. Stone: *Surface-launched Acoustic Wave Sensors: Chemical Sensing and Thin-film Characterization* (Wiley-Interscience, New York, 1997).
- 18 V. B. Raj, A. T. Nimal, Y. Parmar, M. U. Sharma, K. Sreenivas, and V. Gupta: *Sens. Actuators, B* **147** (2010) 517. <https://doi.org/10.1016/j.snb.2010.03.079>
- 19 D. Li, X. Zu, D. Ao, Q. Tang, Y. Fu, Y. Guo, K. Bilawal, M. B. Faheem, L. Li, S. Li, and Y. Tang: *Sens. Actuators, B* **294** (2019) 55. <https://doi.org/10.1016/j.snb.2019.04.010>
- 20 D. Li, Y. Tang, D. Ao, X. Xiang, S. Wang, and X. Zu: *Int. J. Hydrogen Energy* **44** (2019) 3985. <https://doi.org/10.1016/j.ijhydene.2018.12.083>

- 21 S. Wang, J. Ma, Z. Li, H. Q. Su, N. R. Alkurd, W. Zhou, L. Wang, B. Du, Y. Tang, D. Ao, S. Zhang, Q. K. Yu, X. Zu: *J. Hazard. Mater.* **285** (2015) 368. <https://doi.org/10.1016/j.jhazmat.2014.12.014>
- 22 X. Chen, D. M. Li, S. F. Liang, S. Zhan, and M. Liu: *Sens. Actuators, B* **177** (2013) 364. <https://doi.org/10.1016/j.snb.2012.10.120>
- 23 P. G. Su and L. Y. Yang: *Sens. Actuators, B* **223** (2016) 202. <https://doi.org/10.1016/j.snb.2015.09.091>
- 24 J. Gong, Y. Li, Z. Hu, and Y. Deng: *J. Phys. Chem. C* **114** (2010) 9970. <https://doi.org/10.1021/jp100685r>
- 25 H. Tai, Y. Jiang, G. Xie, J. Yu, and M. Zhao: *Int. J. Environ. Anal. Chem.* **87** (2007) 539. <https://doi.org/10.1080/03067310701272954>
- 26 Y. Wang, W. Jia, T. Strout, A. Schempf, H. Zhang, B. Li, J. Cui, and Y. Lei: *Electroanalysis* **21** (2009) 1432. <https://doi.org/10.1002/elan.200904584>
- 27 T. Sugimoto and T. Kojima: *J. Phys. Chem. C* **112** (2008) 18760. <https://doi.org/10.1021/jp8029506>
- 28 F. P. Belleville and H. G. Floch: *SPIE's 1994 Int. Symp. Optics, Imaging, and Instrumentation (SPIE, 1994)* 25–32.

